
This is an electronic reprint of the original article.
This reprint may differ from the original in pagination and typographic detail.

Van Uytven, Wim; Dekeyser, Wouter; Blommaert, Maarten; Horsten, Niels; Baelmans, Martine

Effect of drifts and currents on the validity of a fluid model for the atoms in the plasma edge

Published in:
Nuclear Materials and Energy

DOI:
[10.1016/j.nme.2022.101255](https://doi.org/10.1016/j.nme.2022.101255)

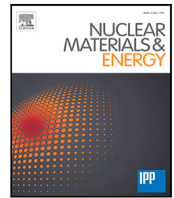
Published: 01/10/2022

Document Version
Publisher's PDF, also known as Version of record

Published under the following license:
CC BY-NC-ND

Please cite the original version:
Van Uytven, W., Dekeyser, W., Blommaert, M., Horsten, N., & Baelmans, M. (2022). Effect of drifts and currents on the validity of a fluid model for the atoms in the plasma edge. *Nuclear Materials and Energy*, 33, Article 101255. <https://doi.org/10.1016/j.nme.2022.101255>

This material is protected by copyright and other intellectual property rights, and duplication or sale of all or part of any of the repository collections is not permitted, except that material may be duplicated by you for your research use or educational purposes in electronic or print form. You must obtain permission for any other use. Electronic or print copies may not be offered, whether for sale or otherwise to anyone who is not an authorised user.



Effect of drifts and currents on the validity of a fluid model for the atoms in the plasma edge

Wim Van Uytven^{a,*}, Wouter Dekeyser^a, Maarten Blommaert^b, Niels Horsten^{a,c}, Martine Baelmans^a

^a KU Leuven, Department of Mechanical Engineering, Celestijnenlaan 300A, 3001 Leuven, Belgium

^b KU Leuven, Department of Mechanical Engineering, Kleinhoefstraat 4, 2440 Geel, Belgium

^c Department of Applied Physics, Aalto University, Espoo, Finland

ARTICLE INFO

Keywords:

Plasma-edge modeling
Fluid neutral atoms
Drifts & currents
Ion-neutral current
Alcator C-mod

ABSTRACT

The performance of advanced fluid neutral models for the simulation of deuterium atoms in the plasma edge of magnetically confined fusion devices is tested for the first time on cases that include drifts and currents in the plasma model, on a simplified Alcator C-mod case. The unadapted advanced fluid neutral model already gives quantitative agreement, with 5–30% fluid-kinetic discrepancy in the broad vicinity of the strikepoint. A new advective perpendicular transport term is proposed, which further reduces the fluid-kinetic discrepancies for cases with drifts. It is also shown that the ion-neutral current can be calculated consistently for fluid or kinetic neutrals, at least when only atoms are considered. However, its effect on the solution is very small for the studied case.

1. Introduction

To reliably predict the peak heat fluxes and particle loads on the plasma-facing components of fusion devices, accurate plasma-edge models are needed, which require both an accurate plasma model and accurate modeling of neutral particles. In mean-field codes such as SOLPS-ITER [1], the inclusion of drifts and currents in the plasma model allows achieving better agreement between code and experiment, in particular with respect to observed inner–outer divertor asymmetries [2,3]. In recent years, despite the higher computational requirements, including drifts is becoming more common, for example for predictive modeling of ITER [4,5].

For the neutral particles, a kinetic Monte Carlo (MC) treatment is typically used. The EIRENE code [6] is used as the kinetic neutral solver in SOLPS-ITER. This MC treatment, however, becomes computationally expensive in high-recycling and detached regimes due to the resonant charge-exchange (CX) process between hydrogenic atoms and ions. The expensive MC treatment can be partially avoided by using fluid or hybrid fluid-kinetic models for the atoms. However, traditional fluid models could in the past never achieve strong quantitative agreement with the kinetic counterpart, even for cases without drifts. This disagreement made it hard to formulate conclusions on the drift-compatibility of the fluid neutral models [7]. Only in recent years, significant progress has been made on the development of advanced fluid neutral (AFN) models, which now offer an accurate, noise-free,

and computationally efficient alternative for the kinetic treatment [8, 9]. These AFN models concern only the (neutral) atoms, but they can be consistently coupled to a kinetic model for molecules [10,11]. However, these AFN models have been developed in conjunction with plasma edge models that did not include drifts and currents.

In this work, we study for the first time the performance of the AFN models on a case with drifts. On a case with only atoms, we show that the unadapted AFN model already performs well. Next, we propose an additional advective neutral term related to the plasma drifts, which further improves the agreement. Furthermore, we show that the ion-neutral current can be calculated consistently using either fluid or kinetic neutral models, but that it has a very small effect on the solution. The presented work is performed in the new extended grids version of the SOLPS-ITER code suite [12].

2. Model description

2.1. Plasma model

In this work, we focus on a single-species hydrogenic plasma. SOLPS-ITER solves balance equations for the ion particle density, ion parallel velocity, ion temperature, electron temperature, and a current continuity equation to calculate the electrostatic potential. Parallel transport is based on Braginskii [13], but flux-limited. Cross-field

* Corresponding author.

E-mail address: wim.vanuytven@kuleuven.be (W. Van Uytven).

transport is modeled through diffusion coefficients for the anomalous turbulent transport, and through electromagnetic drift velocities. Imbalances in the fluxes for ions and electrons give rise to currents. The potential equation then mandates that the divergence of the currents is zero, such that the plasma remains quasi-neutral. The description of drifts and currents in SOLPS-ITER is based on Ref [14].

Including the self-consistent description of drifts and currents is becoming more commonplace in recent years, among others thanks to dedicated efforts to speed-up these simulations [15]. However, these simulations are still routinely plagued by smaller timesteps or complex convergence issues, which is why plasma-edge simulations without drifts and currents are still being performed. In this case, the drift velocities are turned off, the currents are not computed, and the potential is set to $3.1 T_e/q$, where T_e is the electron temperature and q is the elementary charge. Alternatively, the drifts are turned off, and only the parallel current and potential equation are solved. This simplification can already lead to an improved solution without reducing the timestep.

2.2. Atom modeling

In this paper, we only consider fluid models for hydrogenic atoms in the plasma edge. These are expected to show fluid behavior in highly-collisional regimes due to the resonant charge-exchange reaction. Three collisional processes are considered in the underlying kinetic equation: ionization, recombination (both three-body and radiative), and charge-exchange. Molecules are not simulated explicitly. To approximately take their effect into account, the fraction of thermally released molecules is calculated, but it is then assumed that they immediately dissociate into atoms at the target, as explained in Refs. [8,16,17]. This assumption is made for both the fluid and kinetic approach. Including molecules is regarded as future work. Elastic collisions between atoms, molecules and ions are not yet included in the AFN models and are also regarded as future work.

2.2.1. Kinetic atom model

The kinetic atom model used in this work is identical to that of Refs. [9,17]. The kinetic Boltzmann equation for the phase-space distribution $f_a(\mathbf{r}, \mathbf{v}, t)$ of the atoms (subscript ‘‘a’’) can be written as

$$\frac{\partial}{\partial t} f_a(\mathbf{r}, \mathbf{v}, t) + \mathbf{v} \cdot \nabla f_a(\mathbf{r}, \mathbf{v}, t) = Q_a(\mathbf{r}, \mathbf{v}, t), \quad (1)$$

where \mathbf{r} and \mathbf{v} indicate the position and velocity vector, respectively. Q_a represents all sinks and sources of kinetic atoms due to surface processes, and sources and collisions in the volume. This kinetic equation is 7-dimensional (6 for the steady-state solution), making it too expensive to solve with deterministic methods. Instead, particle-tracing Monte Carlo codes such as EIRENE are typically used. Atoms are created at source locations (gas puffs, volume recombination, recycling surfaces, etc.) and are traced while they travel through the plasma until their ionization. When particles hit a wall element they can either be fast reflected as an atom, thermally released as a molecule, or absorbed at the wall. In this work, the molecules are assumed to dissociate immediately at the targets, as explained above. When kinetic particles collide with (or ionize to) the plasma, source terms for particles, parallel momentum, and energy are calculated and transferred to the plasma equations.

2.2.2. Advanced fluid neutral model

The fluid equations for the atoms consist of partial differential equations for the conservation of mass, parallel momentum, and energy. The atom continuity equation is given by

$$\frac{\partial n_a}{\partial t} + \nabla \cdot \Gamma_a^n = S_a^n. \quad (2)$$

Here, n_a is the atom density, Γ_a^n is the atom particle flux, and S_a^n is the atom particle source term. The latter is determined by the recombination and ionization processes:

$$S_a^n = n_i n_e K_r - n_a n_e K_i, \quad (3)$$

where K_r and K_i are the rate coefficient for volume recombination and ionization, respectively, and n_i and n_e are the ion and electron particle densities ($n_i = n_e$ in case of a single-species hydrogenic plasma). To obtain the particle flux Γ_a^n , we need to solve the momentum equation. The full momentum equation is given by

$$m \frac{\partial(n_a \mathbf{V}_a)}{\partial t} + \nabla \cdot (m n_a \mathbf{V}_a \mathbf{V}_a + \Pi_a) = -\nabla p_a + S_a^m. \quad (4)$$

Here, \mathbf{V}_a is the atom bulk velocity vector, Π_a is the stress tensor, p_a is the atom pressure, and S_a^m is the atom momentum source due to interaction with the plasma, given by

$$S_a^m = m((n_i n_e K_r + n_a n_i K_{CX,m}) \mathbf{V}_i - (n_e n_a K_i + n_i n_a K_{CX,m}) \mathbf{V}_a), \quad (5)$$

where $K_{CX,m}$ the momentum-linearized CX rate coefficient, as defined in Ref. [8], and \mathbf{V}_i is the ion velocity vector. Currently, SOLPS-ITER does not solve the full 3D momentum equation. Only for the parallel momentum a conservation equation is solved, while for the perpendicular directions, expressions for fluxes or velocities must currently be explicit.

Close to the targets, important differences between the ion and atom parallel velocity exist due to the recycling and reflection physics, as will be shown in Fig. 3. In the majority of the domain, the ion and atom parallel velocities will equilibrate due to the strong CX interaction. The ion parallel velocities are much higher than the perpendicular ones, especially in the absence of drifts. Hence, for the perpendicular directions, the LHS terms in Eq. (4) are assumed to be small, and the transport of atoms is expected to be dominated by a static force balance between the pressure gradient and the ion–atom momentum exchange. This assumption then leads to:

$$m((n_i n_e K_r + n_a n_i K_{CX,m}) \mathbf{V}_{i,\perp} - (n_e n_a K_i + n_i n_a K_{CX,m}) \mathbf{V}_{a,\perp}) = \nabla_{\perp} p_a. \quad (6)$$

Here, \perp represents both perpendicular directions when used in vector context ($\Phi_{\perp} = 0 \hat{\mathbf{e}}_{\parallel} + \Phi_{\perp} \hat{\mathbf{e}}_{\perp} + \Phi_r \hat{\mathbf{e}}_r$), while \perp and r represent the diamagnetic and radial direction, respectively, in a scalar context. Rearranging terms allows to formulate explicit expressions for the perpendicular atom particle flux components:

$$\Gamma_{a,\perp}^n = n_{a,eq} \mathbf{V}_{i,\perp} - D_a^p \nabla_{\perp} p_a. \quad (7)$$

The equilibrium atom density is given by

$$n_{a,eq} = \frac{n_i n_e K_r + n_a n_i K_{CX,m}}{n_i K_{CX,m} + n_e K_i}, \quad (8)$$

and the pressure-diffusion coefficient is given by

$$D_a^p = \frac{1}{m(n_i K_{CX,m} + n_e K_i)}. \quad (9)$$

The latter can also be written as $D_a^p = \tau_a/m$, with $\tau_a = (n_i K_{CX,m} + n_e K_i)^{-1}$ the collision time of the atoms.

When keeping only the ExB and diamagnetic drifts for $\mathbf{V}_{i,\perp}$, the poloidal component of the atom particle flux becomes

$$\Gamma_{a,\theta}^n = n_a b_{\theta} V_{a,\parallel} - D_a^p b_{\theta}^2 \nabla_{\theta} p_a + b_{\theta} n_{a,eq} (V_{i,\perp}^{(ExB)} + V_{i,\perp}^{(dia)}), \quad (10)$$

and the radial component becomes

$$\Gamma_{a,r}^n = -D_a^p \nabla_r p_a + n_{a,eq} (V_{i,r}^{(ExB)} + V_{i,r}^{(dia)}), \quad (11)$$

where $b_{\theta} = \sqrt{1 - b_{\theta}^2}$ with b_{θ} the poloidal magnetic field pitch, and $p_a = n_a T_a$ is the atom pressure, with T_a the atom temperature.

In all previous studies regarding the AFN models, as well as in the standard neutral models historically available in SOLPS-ITER [18], the last terms on the right-hand side of Eqs. (10) and (11) were neglected. This is a logical choice when plasma drifts are not modeled, because

then $\mathbf{V}_{i,\perp}$ contains only anomalous diffusion, which is typically small compared to parallel transport. In this paper we now investigate if including this advective term gives an improvement when electromagnetic drift velocities are included in $\mathbf{V}_{i,\perp}$. Notice that we have still neglected the complete left hand side of Eq. (4) for the perpendicular directions.

To be able to evaluate Eqs. (10) and (11), the parallel atom velocity and the atom temperature are needed. Parallel to the magnetic field, it was found to be indispensable to solve a complete momentum equation, to take into account the ion-atom friction. The atom parallel velocities ($V_{a,\parallel}$) are expected to be high, as they undergo CX with the plasma, of which the parallel velocity is accelerating to sound speed at the targets. Hence, the LHS of Eq. (4) cannot be expected to be negligible. To close the parallel momentum equation, the viscosity is determined based on the Chapman-Enskog method [19], resulting in $\eta_a = p_a \tau_a$.

The atom parallel momentum equation as currently implemented in SOLPS-ITER is a reduced version of the full parallel momentum equation, based on several assumptions, such as $b_\theta \ll 1$, small magnetic field gradients, small gradients of the metric coefficients, and, lastly, $V_{a,\perp} \ll V_{a,\parallel}$ and $V_{a,r} \ll V_{a,\parallel}$ (see the derivation in Chapter 3 of Ref. [20]). When atoms are dragged along with the plasma drifts due to CX, the assumption of $V_{a,\perp} \ll V_{a,\parallel}$ and $V_{a,r} \ll V_{a,\parallel}$ could be violated. The reduced parallel momentum equation is given by

$$m \frac{\partial(n_a V_{a,\parallel})}{\partial t} + \nabla \cdot \mathbf{\Gamma}_a^m + \nabla_{\parallel} p_a = S_{a,\parallel}^m + S_{CF,\parallel}^m. \quad (12)$$

Here, the atom parallel momentum sources due to ion-atom interaction ($S_{a,\parallel}^m$) is given by

$$S_{a,\parallel}^m = m((n_i n_e K_r + n_a n_i K_{CX,m})V_{i,\parallel} - (n_a n_e K_i + n_a n_i K_{CX,m})V_{a,\parallel}), \quad (13)$$

and $S_{CF,\parallel}^m$ is a centrifugal term. The parallel momentum flux is given by $\mathbf{\Gamma}_{a,\parallel}^m = mV_{a,\parallel} \mathbf{\Gamma}_a^n - n_a \nabla V_{a,\parallel}$ which now includes the contribution from drifts in $\mathbf{\Gamma}_a^n$.

Modeling a separate energy equation for the atoms can provide a modest further reduction of the fluid-kinetic discrepancies [8,9,17], but here we assume that $T_a = T_i$. Studying the impact of a separate T_a on the current research is left for future work. When assuming $T_a = T_i$ in SOLPS-ITER simulations with fluid atoms, a combined ion-neutral energy equation is solved, for which the heat fluxes and heat source terms are summed over all ion and atom species, and subsequently solved for a common ion-atom temperature (T_{i+a}). Also here, a contribution due to the drifts now enters the convective heat transport contribution for the atoms. To remain consistent with the code and the code reference equations, we henceforth denote T_{i+a} simply by T_i , but one must keep in mind that T_i represents the true ion temperature when separate ion and atom energy equations are solved with fluid atoms, or when coupling to kinetic atoms, while it represents T_{i+a} when a combined ion-atom energy equation is solved when fluid atoms are used.

The fluid transport model for the atoms described above must be complemented with appropriate boundary conditions. The AFN boundary conditions provide net fluxes of particles, parallel momentum and energy at the grid boundaries, consistent with the recycling and reflection processes included in the kinetic atom model. These boundary conditions are described in detail in Ref. [8], and their implementation in SOLPS-ITER is elaborated in Refs. [16,17].

2.3. Ion-neutral current

Neglecting the inertial terms in the parallel projection of the electron momentum equation leads to an expression for the parallel current. Expressions for drifts and currents are found by taking the cross product of the plasma momentum equations with the magnetic field vector. Most drifts and currents depend only on the plasma quantities (diamagnetic, inertia, and viscosity), except the ion-neutral current which also depends on neutral quantities and is therefore studied in more detail here. The ion-neutral current in SOLPS-ITER follows the derivation of

Rozhansky et al. [21]. We follow the naming convention of Ref. [21] and SOLPS-ITER, denoting the ion-neutral current as $j^{(s)}$, to avoid confusion with the inertial current $j^{(in)}$. For a single-species hydrogenic plasma, the ion-neutral currents are given by $\mathbf{j}^{(s)} = -\mathbf{S}_a^m \times \mathbf{B}/B^2 = \mathbf{S}_i^m \times \mathbf{B}/B^2$, resulting in:

$$j_{\parallel}^{(s)} = 0, \quad j_{\perp}^{(s)} = -\frac{S_{a,r}^m}{B} \text{ and } j_r^{(s)} = +\frac{S_{a,\perp}^m}{B}. \quad (14)$$

Here, $S_{a,r}^m$ and $S_{a,\perp}^m$ are the radial and diamagnetic atom momentum source terms due to interaction with the ions. The dominant contribution to this term is expected to come from the charge-exchange terms, and the dominant E×B and diamagnetic ion drifts. Using these assumptions in Eq. (14) leads to:

$$j_{\theta}^{(s)} = j_{\perp}^{(s)} b_{\phi} = \sigma_{in} \left(-b_{\phi}^2 \nabla_{\theta} \Phi - b_{\phi}^2 \frac{1}{n_i q} \nabla_{\theta} (n_i T_i) + B_{\phi} V_{a,r} \right), \quad (15)$$

and

$$j_r^{(s)} = \sigma_{in} \left(-\nabla_r \Phi - \frac{1}{n_i q} \nabla_r (n_i T_i) - B V_{a,\perp} \right), \quad (16)$$

where the ion-neutral conductivity is given by

$$\sigma_{in} = \frac{m_i n_i n_a K_{CX,m}}{B^2}. \quad (17)$$

$V_{a,\perp}$ and n_a are calculated on the fluid side of the code (B2.5) in the case of fluid neutral models. For kinetic simulations, if radial and diamagnetic momentum exchange were scored in EIRENE, $\mathbf{j}^{(s)}$ could be calculated directly from Eq. (14), allowing to also take into account the momentum sources due to interactions with molecules. Since the radial and diamagnetic momentum source are currently not scored in EIRENE, Eqs. (15) and (16) are used, with $V_{a,\perp}$ and n_a obtained from post-processing the EIRENE simulation and $K_{CX,m}$ from the B2.5 side.

3. Application to Alcator C-mod case

We apply the models from the previous section to a simplified Alcator C-mod case. This device was selected because it is a small machine, where the drifts are known to have a large effect on the solution, and because it operates at high densities compared to other devices of similar size, leading to conditions of high collisionality where the assumptions of the fluid neutral model are satisfied. Both these aspects will facilitate to draw conclusions regarding the drift-compatibility of the AFN models.

3.1. Case set-up

While we use the geometry of Alcator C-mod [22], we do not simulate a particular experimental shot. Rather, we focus on the use of either a fluid or kinetic model for the atoms. The finite volume grid used in this study is given in Fig. 1. It consists of 30 cells in the radial direction and 80 cells in the poloidal direction. The grid is poloidally refined towards the targets (< 1 mm), to achieve a low discretization error in the regions of highest ion-neutral interaction. The void regions, which are the regions between the plasma grid and the actual vessel wall, where kinetic neutrals are typically still simulated, are removed. This way, the models with fluid atoms can be compared to those with kinetic neutrals on an identical grid. Spatially hybrid fluid-kinetic neutral models to include the void regions are already available [10,11,23], but they are not used here.

For the plasma model, we use an anomalous particle transport coefficient $D^n = 0.3 \text{ m}^2 \text{ s}^{-1}$, ion/electron heat conductivity coefficients $\chi_i = \chi_e = 1.5 \text{ m}^2 \text{ s}^{-1}$ and an ion viscosity coefficient $\eta_i = 0.2 \text{ m}^2 \text{ s}^{-1}$. At the core, T_e and T_i are fixed at 170 and 175 eV, respectively, and the core plasma density is fixed at $1.61 \cdot 10^{20} \text{ m}^{-3}$. At the private flux boundaries, an absorption coefficient of 5% is applied for the incident atoms. For the plasma model with drifts, the drifts are activated (forward field, with the ion grad-B drift pointing down), and all currents are turned on, except for the electric current connected with the contribution of the

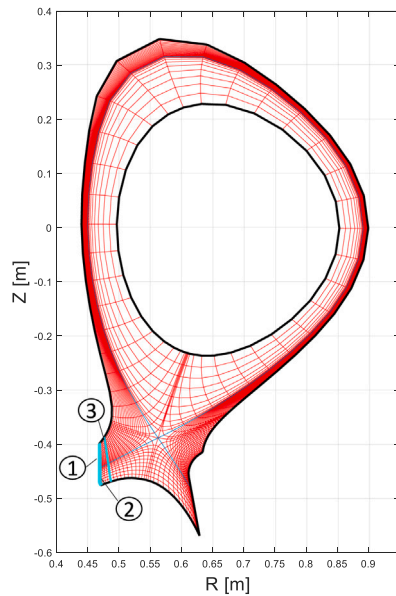


Fig. 1. Alcator C-mod computational grid without void regions. Three radial lines in the inner divertor leg are indicated in cyan, along which atom and plasma quantities are plotted in Figs. 3 and 4. (For interpretation of the references to color in this figure legend, the reader is referred to the web version of this article.)

perpendicular viscosity ($\tilde{\nu}^{(vis\perp)}$ in SOLPS-ITER), which is not yet fully implemented in the new extended grids SOLPS-ITER code. Also, the ion-neutral current is not yet included in the results of Figs. 2–4, but it is activated and studied separately in Section 3.4. Only the steady-state solutions are studied here.

3.2. Results with unadapted AFN model

In a first step, we compare the results for four different models: with and without plasma drifts, and using either a kinetic atom model or the unadapted fluid atom model. Fig. 2 displays target profiles of the converged solutions. A first observation is that the drifts have a large effect on the solution. Without drifts, both targets have a density peak of $4 - 6 \cdot 10^{19} \text{ m}^{-3}$, slightly outward from the strikepoint. The ion temperature remains at 1–2 eV in the private flux region and increases to 15–30 eV outward from the strikepoint. With drifts included, the density peak shifts upward on the inner target and the density stays above $2 \cdot 10^{19} \text{ m}^{-3}$ all the way up to the main chamber wall, and the ion temperature remains below 2 eV along the entire inner target. On the outer target, two density peaks now exist, one in the private flux region and one in the SOL. These trends correspond qualitatively to the findings of earlier SOLPS-ITER modeling efforts of Alcator C-mod [24]. These trends are captured qualitatively by both the kinetic and unadapted AFN model. The precise quality of the fluid-kinetic agreement depends for a large part on the Knudsen number (Kn), with $\text{Kn} = \lambda_{\text{CX}}/L$, where λ_{CX} is the CX mean free path of the atoms, and L is a macroscopic length scale of the problem. Here, we have modeled L as a scalar constant, representative of an average of the gradient length scales of density and temperature at the divertor targets, which was observed to be $\approx 0.02 \text{ m}$. When $\text{Kn} < 0.01$, the fluid approach is strictly valid, while for $\text{Kn} < 0.1$ good agreement can be expected. For $0.1 < \text{Kn} < 1$ discrepancies will become substantial and for $\text{Kn} > 1$ strong kinetic effects will make the fluid approach invalid. From plotting Kn along the inner and outer target, it is immediately clear that the fluid model cannot be expected to be fully valid. $\text{Kn} < 0.1$ is only achieved near the strikepoint on the inner target, while a large part of the targets has $0.1 < \text{Kn} < 1$. Hence, at least part of the fluid-kinetic discrepancy in Fig. 2 is due to the fact that collisionality is not high enough for the fluid approach to be fully valid.

3.3. Influence of drifts on atom velocities

We start from the plasma background obtained by converging the plasma model with drifts coupled to the unadapted fluid atom model. On this background (n_i, n_e, T_i, T_e, V_i), the kinetic solution is calculated by running a single EIRENE simulation with a large number of particles (denoted by “MC-D”, where D stands for “drift”). Next, we recalculate the MC solution on a plasma background with the same n_i, n_e, T_i, T_e and $V_{i,\parallel}$, but the drift velocities are removed from $V_{i,\theta}$ and $V_{i,r}$ in the plasma background which is passed to EIRENE (denoted by “MC-ND”, where ND stands for “no drift”). This way, we can isolate the effect of drift velocities on the atoms from the effect of drifts on the plasma equations themselves. On the same plasma background with drifts, we also calculate the unadapted AFN solution, which does not include the $n_{a,eq} V_{i,\perp}$ term in Eq. (7), and also the adapted AFN model, which does take this term into account. Fig. 3 compares the atom solutions (density, diamagnetic velocity, radial velocity, and parallel velocity) for the four different models. Generally, qualitative agreement is achieved for all models.

The parallel velocities of the atoms agree very well for all four models. This means that adding more terms in the parallel momentum equation, as mentioned in Section 2.2.2, can yield only marginal improvements. The largest fluid-kinetic discrepancies are instead found for $V_{a,\perp}$ and $V_{a,r}$ close to the target below the strikepoint (encircled in magenta). However, these appear to be inherent fluid-kinetic discrepancies, and the plasma drifts have no influence on this discrepancy. Radially outward, however, noticeable differences due to the plasma drifts exist, for both the fluid and kinetic case (encircled in green). Including the drift-advective term in the fluid atom model (“AFN-unadapt” → “AFN-adapt”) leads to a similar correction of the solution as when including the drifts for the kinetic atom model (“MC-ND” → “MC-D”). When the drift-advective term is included, the fluid-kinetic discrepancies are not larger than they were without drifts.

Next, Fig. 4 shows density and temperature profiles along the inner target, and 20 mm upstream of the inner target. At the target itself, the influence of including the drift velocities in the atom simulation is small. 20 mm upstream of the target, however, the differences become visually clear. Both for the density and ion temperature, it is clear that the inclusion of the advective term in the AFN models reduces the fluid-kinetic discrepancies. Moreover, the differences between the unadapted AFN model and the “MC-ND” model are similar to the differences between the adapted AFN model and the “MC-D” model. This observation again confirms that after the inclusion of the drift-advective terms in the AFN model, the fluid-kinetic discrepancies are no larger than they were for the cases without drifts.

In the outer divertor leg (not shown in the plot), the fluid-kinetic discrepancies are larger, due to higher Knudsen numbers (see Fig. 2), but there is almost no influence of drifts on the atoms, for neither the kinetic nor fluid models.

In theory, many terms could be added to the fluid atom model for the state equations and for the boundary conditions, if we cannot assume that $V_{a,\perp} \ll V_{a,\parallel}$ and $V_{a,r} \ll V_{a,\parallel}$ (see the derivations in Ref. [8] and Chapters 3 and 4 of Ref. [20]). However, the results from Figs. 2–4 show that the presented AFN models already capture the dominant physical processes for the atoms well. If the reduction in fluid-kinetic discrepancy that any additional fluid terms could provide is not significantly larger than the inherent fluid-kinetic discrepancies which are present because $\text{Kn} < 0.1$ does not hold everywhere, then it is potentially much more efficient to correct for these terms using hybrid fluid-kinetic models (see Refs. [11,25–27] for the different types of hybrid fluid-kinetic methods under development), rather than further complicating the fluid models themselves.

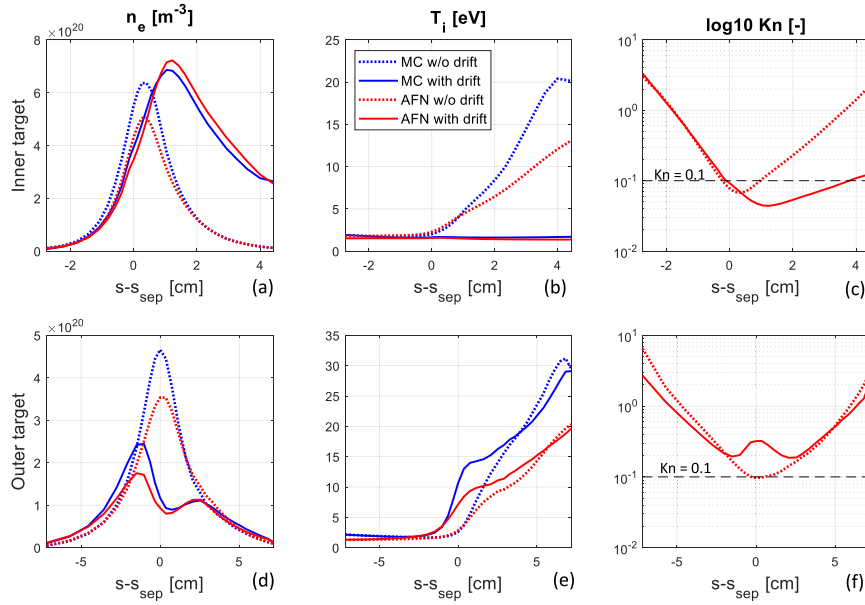


Fig. 2. Plasma density, ion temperature and Knudsen number along the inner target ((a)–(c)) and outer target ((d)–(f)) obtained by using either a plasma model without drifts (dashed lines) or with drifts (full lines), and using either kinetic MC atoms (blue) or the unadapted AFN model (red). (For interpretation of the references to color in this figure legend, the reader is referred to the web version of this article.)

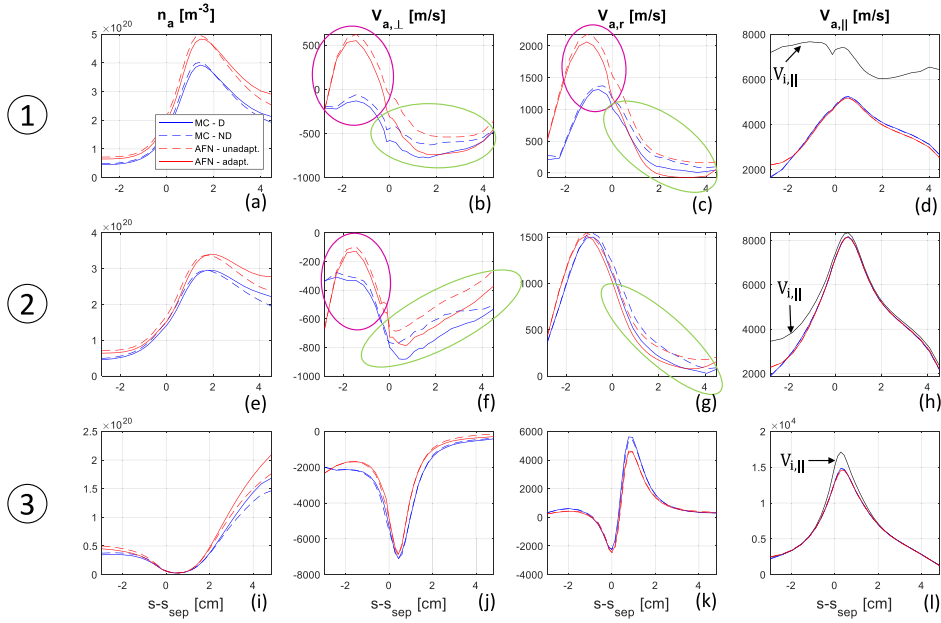


Fig. 3. Atom density, diamagnetic atom velocity, radial atom velocity, and parallel atom velocity along the inner target ((a)–(d)), ± 3 mm in front of the inner target ((e)–(h)), and ± 20 mm in front of the inner target ((i)–(l)), corresponding to the radial lines indicated in Fig. 1. The kinetic solution on a plasma background with drifts (blue full lines), the kinetic solution on the same plasma background, but with drift velocities removed (blue dashed lines), the unadapted AFN model (red dashed lines), and the AFN model with the advective term of Eq. (7) included (red full line) are compared. The ion parallel velocity of the fixed plasma background is also shown (black full lines). (For interpretation of the references to color in this figure legend, the reader is referred to the web version of this article.)

3.4. Effect of ion-neutral current

Fig. 5 displays the ion-neutral current densities. It is concluded that the fluid and kinetic treatment agree excellently. This is in part due to the fact that the atom density and velocities agree reasonably well (as was shown in Section 3.3), but also because $K_{CX,m}$ is always computed on the B2.5 side.

The impact of this current on the coupled solution appears to be very limited for the studied case. It is clear from Fig. 6 that the ion-neutral current has only a very small effect at the inner target ($< 2\%$), and the maximum relative difference on the plasma density

across the entire domain is 9% for the kinetic reference solution. This conclusion is limited, however, by the single simplified Alcator C-mod case performed here. It should be verified in the future whether the effect of the ion-neutral current remains small in reactor-relevant divertors.

4. Conclusions and future work

The effect of drifts and currents on the validity of atom-only fluid models was studied on a simplified Alcator C-mod case. It was found that the drifts have an observable effect on the atoms, due to higher

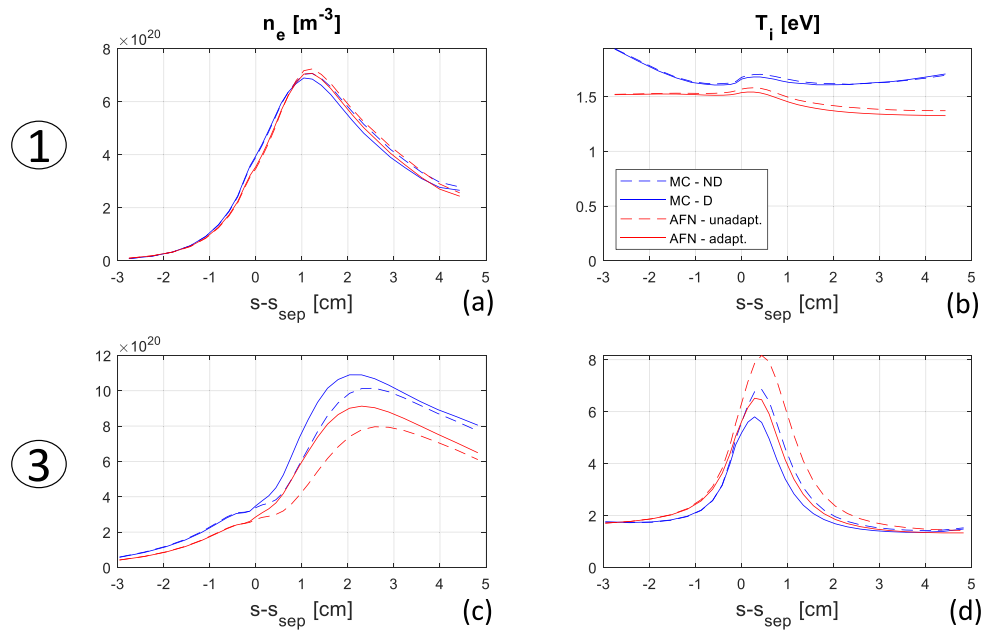


Fig. 4. Plasma density and ion temperature along the inner target ((a) and (b)), and ± 20 mm in front of the inner target ((c) and (d)) of the coupled solutions. The plasma model with drifts is coupled to either kinetic atoms (solid blue lines), kinetic atoms, but with the drift velocities removed from the EIRENE background (blue dashed lines), unadapted AFN model (red dashed lines), and adapted AFN model (solid red line). (For interpretation of the references to color in this figure legend, the reader is referred to the web version of this article.)

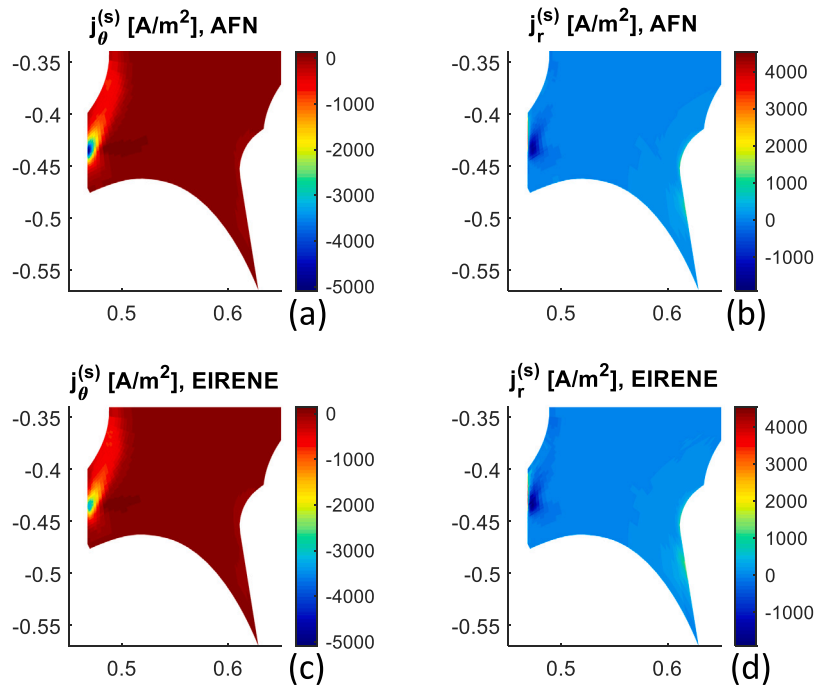


Fig. 5. Ion-neutral current density computed on a fixed plasma background coupled to either the AFN model ((a)–(b)) or EIRENE ((c)–(d)) in the poloidal ((a) and (c)), and radial ((b) and (d)) direction.

perpendicular velocities with which the atoms collide, but the effect was not very large, with relative differences $< 5\%$ in large parts of the computational domain and a maximum relative difference of 15% on the plasma density of the coupled solution. Therefore, the unadapted fluid neutral models already showed good agreement with the kinetic neutral solution.

In this paper, we proposed an additional term to take into account that the atoms will be partially “dragged along” by the plasma drifts in the perpendicular directions. It was shown that adding this term further reduces the fluid-kinetic discrepancies. It was argued that it is

potentially more efficient to address the remaining discrepancies using hybrid fluid-kinetic methods, rather than further complicating the fluid atom models themselves.

Next, it was shown that the ion-neutral current can be calculated consistently for either fluid or kinetic neutrals, at least when only atoms are considered. However, the contribution from the ion-neutral current to the coupled solution was found to be very small. In future work, it should be checked if the same conclusion holds for reactor-sized machines, such as ITER and DEMO.

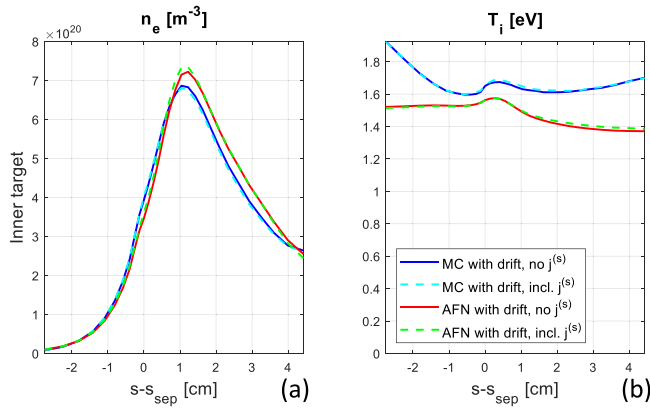


Fig. 6. Inner target profiles of plasma density (a) and ion temperature (b) obtained with the plasma model with drifts using either kinetic MC atoms but no ion-neutral current (blue full line), kinetic atoms but with ion-neutral current (cyan dashed line), fluid atoms without ion-neutral current (red full line), or fluid atoms with ion-neutral current (green dashed line). (For interpretation of the references to color in this figure legend, the reader is referred to the web version of this article.)

The importance of the effect of the plasma drifts on the neutral solution can be easily checked for kinetic neutrals, by turning off the drifts in the background which is passed to the kinetic neutral solver, and comparing it with the standard solution. If cases are encountered where these difference are much larger than those found in this paper, the work regarding the drift-compatibility of fluid neutral models should be further elaborated, and the models presented here can then serve as a starting point.

Regarding future work, the presented models can be extended with a kinetic simulation of the molecules, as was done in Refs. [10,11], but this does not require additional model development. Towards ITER and DEMO simulations, the inclusion of elastic collisions between atoms, molecules and ions in the AFN models should be considered.

CRediT authorship contribution statement

Wim Van Uytven: Conceptualization, Methodology, Software, Validation, Investigation, Writing – original draft, Writing – review & editing, Visualization, Formal analysis. **Wouter Dekeyser:** Conceptualization, Methodology, Software, Writing – review & editing, Supervision, Data curation. **Maarten Blommaert:** Conceptualization, Methodology, Writing – review & editing, Supervision. **Niels Horsten:** Conceptualization, Methodology, Writing – review & editing. **Martine Baelmans:** Conceptualization, Methodology, Writing – review & editing, Supervision.

Declaration of competing interest

The authors declare that they have no known competing financial interests or personal relationships that could have appeared to influence the work reported in this paper.

Data availability

Data will be made available on request.

Acknowledgments

The first author is funded by a PhD fellowship of the Research Foundation - Flanders. Parts of this work have been carried out within the framework of the EUROfusion Consortium, funded by the European Union via the Euratom Research and Training Programme (Grant

Agreement No 101052200 — EUROfusion). Views and opinions expressed are however those of the author(s) only and do not necessarily reflect those of the European Union or the European Commission. Neither the European Union nor the European Commission can be held responsible for them. The computational resources and services used in this work were provided by the VSC (Flemish Supercomputer Center), funded by the Research Foundation Flanders (FWO) and the Flemish Government - department EWI.

References

- [1] S. Wiesen, D. Reiter, V. Kotov, M. Baelmans, W. Dekeyser, A. Kukushkin, S. Lisgo, R. Pitts, V. Rozhansky, G. Saibene, et al., The new SOLPS-ITER code package, *J. Nucl. Mater.* 463 (2015) 480–484.
- [2] I. Pérez, M. Groth, M. Wischmeier, D. Coster, D. Brida, P. David, D. Silvagni, M. Faitsch, A.-U. Team, E.M. Team, Impact of drifts in the ASDEX upgrade upper open divertor using SOLPS-ITER, *Contrib. Plasma Phys.* 60 (5–6) (2020) e201900166.
- [3] W. Dekeyser, X. Bonnin, S. Lisgo, R. Pitts, B. LaBombard, Implementation of a 9-point stencil in SOLPS-ITER and implications for Alcator C-Mod divertor plasma simulations, *Nucl. Mater. Energy* 18 (2019) 125–130.
- [4] E. Kaveeva, V. Rozhansky, I. Senichenkov, E. Sytova, I. Veselova, S. Voskoboynikov, X. Bonnin, R. Pitts, A. Kukushkin, S. Wiesen, et al., SOLPS-ITER modelling of ITER edge plasma with drifts and currents, *Nucl. Fusion* 60 (4) (2020) 046019.
- [5] I. Veselova, E. Kaveeva, V. Rozhansky, I. Senichenkov, A. Poletaeva, R. Pitts, X. Bonnin, SOLPS-ITER drift modelling of ITER burning plasmas with narrow near-SOL heat flux channels, *Nucl. Mater. Energy* 26 (2021) 100870.
- [6] D. Reiter, M. Baelmans, P. Börner, The EIRENE and B2-EIRENE codes, *Fusion Sci. Technol.* 47 (2) (2005) 172–186.
- [7] K. Hoshino, M. Toma, A. Hatayama, D. Coster, X. Bonnin, R. Schneider, H. Kawashima, N. Asakura, Y. Suzuki, Benchmarking kinetic and fluid neutral models with drift effects, *Contrib. Plasma Phys.* 48 (1–3) (2008) 136–140.
- [8] N. Horsten, G. Samaey, M. Baelmans, Development and assessment of 2D fluid neutral models that include atomic databases and a microscopic reflection model, *Nucl. Fusion* 57 (11) (2017) 116043.
- [9] W. Van Uytven, M. Blommaert, W. Dekeyser, N. Horsten, M. Baelmans, Implementation of a separate fluid-neutral energy equation in SOLPS-ITER and its impact on the validity range of advanced fluid-neutral models, *Contrib. Plasma Phys.* 60 (5–6) (2020) e201900147.
- [10] N. Horsten, M. Groth, M. Blommaert, W. Dekeyser, I.P. Pérez, S. Wiesen, J. Contributors, Application of spatially hybrid fluid-kinetic neutral model on JET L-mode plasmas, *Nucl. Mater. Energy* 27 (2021) 100969.
- [11] W. Van Uytven, W. Dekeyser, M. Blommaert, N. Horsten, Y. Marandet, M. Baelmans, Advanced spatially hybrid fluid-kinetic modelling of plasma-edge neutrals and application to ITER case using SOLPS-ITER, *Contrib. Plasma Phys.* (2022) e202100191.
- [12] W. Dekeyser, P. Börner, S. Voskoboynikov, V. Rozhansky, I. Senichenkov, E. Kaveeva, I. Veselova, E. Vekshina, X. Bonnin, R. Pitts, et al., Plasma edge simulations including realistic wall geometry with SOLPS-ITER, *Nucl. Mater. Energy* 27 (2021) 100999.
- [13] S. Braginskii, M. Leontovich, *Reviews of Plasma Physics*, Consultants Bureau New York, 1965.
- [14] V. Rozhansky, E. Kaveeva, P. Molchanov, I. Veselova, S. Voskoboynikov, D. Coster, G. Counsell, A. Kirk, S. Lisgo, M. Team, et al., New B2SOLPS5.2 transport code for H-mode regimes in tokamaks, *Nucl. Fusion* 49 (2) (2009) 025007.
- [15] E. Kaveeva, V. Rozhansky, I. Senichenkov, I. Veselova, S. Voskoboynikov, E. Sytova, X. Bonnin, D. Coster, Speed-up of SOLPS-ITER code for tokamak edge modeling, *Nucl. Fusion* 58 (12) (2018) 126018.
- [16] M. Blommaert, W. Dekeyser, N. Horsten, P. Börner, M. Baelmans, Implementation of a consistent fluid-neutral model in SOLPS-ITER and benchmark with EIRENE, *Contrib. Plasma Phys.* 58 (6–8) (2018) 718–724.
- [17] W. Van Uytven, W. Dekeyser, M. Blommaert, S. Carli, M. Baelmans, Assessment of advanced fluid neutral models for the neutral atoms in the plasma edge and application in ITER geometry, *Nucl. Fusion* (2022).
- [18] R. Schneider, X. Bonnin, K. Borrass, D. Coster, H. Kastelewicz, D. Reiter, V. Rozhansky, B. Braams, Plasma edge physics with B2-EIRENE, *Contrib. Plasma Phys.* 46 (1–2) (2006) 3–191.
- [19] A. Bobylev, The Chapman-Enskog and Grad methods for solving the Boltzmann equation, in: *Akademiia Nauk SSSR Doklady*, Vol. 262, (1) 1982, pp. 71–75.
- [20] N. Horsten, Fluid and Hybrid Fluid-Kinetic Models for the Neutral Particles in the Plasma Edge of Nuclear Fusion Devices (Ph.D. thesis), KU Leuven, 2019.
- [21] V. Rozhansky, S. Voskoboynikov, E. Kaveeva, D. Coster, R. Schneider, Simulation of tokamak edge plasma including self-consistent electric fields, *Nucl. Fusion* 41 (4) (2001) 387.
- [22] M. Greenwald, A. Bader, S. Baek, M. Bakhtiari, H. Barnard, W. Beck, W. Bergerson, I. Bespamyatnov, P. Bonoli, D. Brower, et al., 20 Years of research on the Alcator C-Mod tokamak, *Phys. Plasmas* 21 (11) (2014) 110501.

- [23] M. Blommaert, N. Horsten, P. Börner, W. Dekeyser, A spatially hybrid fluid-kinetic neutral model for SOLPS-ITER plasma edge simulations, *Nucl. Mater. Energy* 19 (2019) 28–33.
- [24] W. Dekeyser, X. Bonnin, S.W. Lisgo, R.A. Pitts, D. Brunner, B. LaBombard, J.L. Terry, SOLPS-ITER study of neutral leakage and drift effects on the Alcator C-Mod divertor plasma, *Nucl. Mater. Energy* 12 (2017) 899–907.
- [25] N. Horsten, M. Groth, W. Dekeyser, W. Van Uytven, S. Carli, J. Contributors, Combination of micro–macro and spatially hybrid fluid-kinetic approach for hydrogenic plasma edge neutrals, *Contrib. Plasma Phys.* (2022) e202100188.
- [26] B. Mortier, M. Baelmans, G. Samaey, Kinetic-diffusion asymptotic-preserving Monte Carlo algorithms for plasma edge neutral simulation, *Contrib. Plasma Phys.* 60 (5–6) (2020) e201900134.
- [27] M. Valentinuzzi, Y. Marandet, H. Bufferand, G. Ciraolo, P. Tamain, Two-phases hybrid model for neutrals, *Nucl. Mater. Energy* 18 (2019) 41–45.